THE JOURNAL OF BIOLOGICAL CHEMISTRY
Vol. 269, No. 46, Issue of November 18, pp. 28724–28731, 1994
Printed in U.S.A.

Random Chimeragenesis of G-protein-coupled Receptors

MAPPING THE AFFINITY OF THE cAMP CHEMOATTRACTANT RECEPTORS IN *DICTYOSTELIUM**

(Received for publication, May 20, 1994, and in revised form, August 24, 1994)

Ji-Yun Kim and Peter N. Devreotes‡

From the Department of Biological Chemistry, The Johns Hopkins University, School of Medicine, Baltimore, Maryland 21205

G-protein-coupled receptors mediate a wide variety of responses to extracellular stimuli in eucaryotic cells. Binding of the ligand to these receptors is thought to involve contacts within a pocket formed by the seven transmembrane domains inferred from the sequences of these genes. A family of four surface cAMP receptors that mediate responses to secreted cAMP coordinates the developmental program of *Dictyostelium*. A large difference in affinity for cAMP exists between cAR1 (25 and 230 nM) and cAR2 (>5 μM). To understand the basis for this affinity difference, we generated an extensive series of cAR1/cAR2 and cAR2/cAR1 chimeras using a technique designated "random chimeragenesis." When a linearized plasmid was transformed into *Escherichia coli*, tandemly positioned cAR1 and cAR2 genes crossed over at homologous regions. The cAMP binding properties and EC_{50} values for agonist-induced phosphorylation of each of the chimeras were characterized in order to map the domains that determine the affinity. These studies implicated a domain in the second extracellular loop in which only 5 residues differ between the two receptors as the major determinant of affinity. A secondary domain including residues 110–147 (11 residue differences) was identified as a minor determinant of affinity.

The responses to light, odorants, a variety of peptide hormones, neurotransmitters, as well as chemoattractants are mediated by G-protein[1]-coupled receptors which contain seven membrane-spanning domains (reviewed in Refs. 1 and 2). These receptors catalyze the activation of heterotrimeric G-proteins which in turn modulate the functioning of adenylyl cyclases, phosphodiesterases, phospholipases, and ion channels (3–5). Desensitization is associated with phosphorylation of the receptor by specific kinases resulting in an uncoupling from the G-protein and downstream effectors (reviewed in Ref. 1). Current views hold that the seven transmembrane helices of the G-protein-coupled receptor form a compact bundle spanning the membrane and that agonist binding alters critical interactions between the helices, transmitting a conformational changes to the cytoplasmic loops (reviewed in Ref. 6).

The family of cAMP chemoattractant receptors (cARs) in *Dictyostelium* provides an excellent model system for investigating the mechanisms by which agonists induce this transition to an activated state (reviewed in Ref. 7). The four cARs control a cell-cell communication system that plays an essential role at multiple stages in the developmental program of this organism. The program is coordinated by extracellular cAMP that is periodically secreted by cells at oscillation centers. Neighboring cells move toward the centers and in turn secrete more cAMP, propagating the signal as a chemical wave (7, 8). The mound formed by the aggregating cells undergoes further cell differentiation and morphogenesis into a migrating slug and finally a fruiting body consisting of stalk and spore cells (9, 10). Throughout development, cAMP acts as a chemoattractant as well as an inducer of developmentally regulated gene expression (reviewed in Ref. 8).

The ligand binding domain on many G-protein coupled receptors is not readily apparent, since a large fraction of the mass resides in the plane of the membrane. In the case of rhodopsin (11, 12) and α- and β-adrenergic receptors (13–15), the critical ligand-receptor interactions are thought to actually reside within the plane of the membrane and involve the seventh and third transmembrane domains (TM7 and TM3) (reviewed in Ref. 16). In contrast, the binding sites on the luteinizing hormone (17, 18) and thyrotropin receptors (19, 20) are found on the long NH_2-terminal extracellular domains. For other G-protein-coupled receptors, such as those for *N*-formyl peptide (21, 22) and substance K (23, 24), the results are less clear, and multiple transmembrane and loop domains have been implicated in the receptor-agonist interactions.

The four cARs share extensive amino acid sequence homology within the transmembrane domains and interconnecting loops (25, 26).[2] Nevertheless, the cAMP binding characteristics of each receptor differ significantly. The K_d values and EC_{50} values for several agonist-induced responses, such as receptor phosphorylation and Ca^{2+} influx, increase in the order cAR1 < cAR3 < cAR2 (27, 28). Under physiological conditions the EC_{50} values of agonist-induced phosphorylation for cAR1 and cAR2 are 30 nM and 50 μM, respectively (29). Interestingly, the affinities of these receptors are correlated with the stage of expression. cAR1 appears during the early aggregation stage, whereas cAR3 is maximal during the mound stage (26, 30). These are followed by cAR2 and cAR4, expressed exclusively in prestalk cells in the slug and culmination stages, respectively (25).[2]

We took advantage of the large affinity difference between cAR1 and cAR2 to investigate the determinants of affinity of an agonist binding domain. We developed a new technique to generate a random collection of chimeras between cAR1 and cAR2. Our analysis of these chimeras shows that a portion of the second extracellular loop connecting TM4 and TM5 is critical in distinguishing the affinities of cAR1 and cAR2. In α- and β-adrenergic receptors, as well as many chemotactic agonist receptors, the use of chimeric receptors to map major structural domains has produced informative results (13, 21, 22). The technique of "random chimeragenesis" (31) presented here would allow these studies to be greatly extended.

* This work was supported by National Institutes of Health Grant GM34933 (to P. N. D.). The costs of publication of this article were defrayed in part by the payment of page charges. This article must therefore be hereby marked "*advertisement*" in accordance with 18 U.S.C. Section 1734 solely to indicate this fact.

‡ To whom all correspondence should be addressed: Dept. of Biological Chemistry, The Johns Hopkins University, School of Medicine, 725 N. Wolfe St., Baltimore, MD, 21205.

[1] The abbreviations used are: G-protein, guanine nucleotide-binding regulatory protein; cAR, cAMP receptor; G418, Geneticin.

[2] J. M. Louis, H. T. Ginsberg, and A. R. Kimmel, manuscript in preparation.

MATERIALS AND METHODS

Plasmids—The plasmids pJK15 and pJK17, containing the cAR1 and cAR2 genes cloned in tandem, were used to generate the libraries of cAR1/cAR2 and cAR2/cAR1 chimeras. The pJK15 plasmid was constructed by subcloning a *Bam*HI/*Bgl*II fragment of cAR1 cDNA (30) into the *Bam*HI site of pPL1. An *Eco*RI fragment of cAR2 genomic DNA (27) was cloned into the *Eco*RI site of pPL1. pPL1 is a modified Bluescript KS$^+$ (Stratagene) which has a *Bgl*II linker inserted into the *Eco*RV site of Bluescript. pJK17 was constructed similarly to pJK15, except that the order of the genes was reversed. After the random chimeragenesis procedure (see below), all of the resulting chimeras have a 5′-end *Bam*HI and a 3′-end *Bgl*II restriction enzyme sites.

Random Chimeragenesis—1 μg of each "tandem" plasmid was linearized by double digestion at *Sma*I and *Pst*I sites situated between the two genes. After assessing the efficiency of digestion by agarose gel electrophoresis, the enzymes were heat-inactivated at 65 °C for 30 min. The resulting digestion mixtures were transformed into *Escherichia coli* strain JM101 cells by heat shock and plated on ampicillin containing LB plates. Eighteen of the resulting colonies were randomly picked and digested to localize the area of crossover. Two clones from each directional libraries contained the original plasmid and the rest were independent chimeras. PCR primers specific to each receptor gene were used to confirm the location. To determine the precise point of crossover and to ensure the sequence integrity, Sanger sequencing was performed for several hundred base pairs surrounding the site. Each of the cAR1/cAR2 chimeras is designated as "N" followed by a number, and each cAR2/cAR1 chimeras is designated by "C" preceded by a number; the number is the junctional amino acid number in reference to the amino acid sequence of cAR1.

Expression of the Receptor Chimeras—Receptor chimeras in pPL1 based plasmids were digested with *Bam*HI/*Bgl*II and ligated into the *Bgl*II site of pJK1, an extrachromosomal vector containing a neomycin gene as a selection marker (32). Wild-type AX-3 *Dictyostelium* cells were transformed by electroporation (32), and stable transformants were selected and maintained by supplementing the medium with G418 (20 μg/ml, Life Technologies, Inc.). Few endogenous receptors are present in growth stage AX-3 cells (33) providing means to study the expressed chimeras in wild-type background.

Cell Culture Conditions—A single clone from each transformation was expanded and maintained in 100-mm culture dishes. Two or three days prior to the experiments, cells were transferred to shaking suspension in HL-5 with G418. Cells were harvested by washing two times in ice-cold phosphate buffer (PB, 10 mM KH_2PO_4/Na_2HPO_4, pH 6.5) and resuspended in ice-cold PB at the desired density (34).

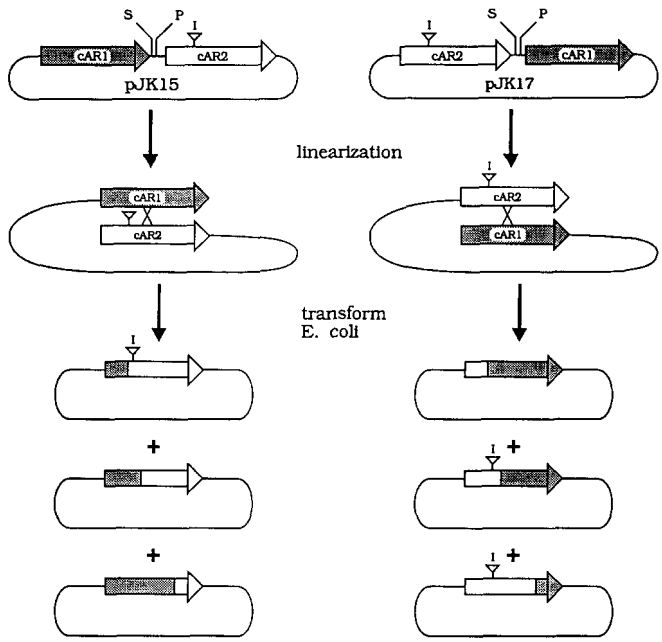

FIG. 1. **Strategy for the random chimeragenesis of receptors.** Plasmids containing wild-type cAR1 cDNA and cAR2 genomic DNA in tandem in the desired order were linearized with restriction endonucleases *Sma*I (*S*) and *Pst*I (*P*) and transformed into *E. coli* strain JM101. Clones were randomly picked to characterize crossover positions. The *stripped bar* symbolizes cAR1 sequence, and the *white bar* indicates cAR2 sequence. "*I*" indicates a 107-base pair intron present in cAR2 genomic DNA.

TABLE I
Single dose cAMP binding

Single dose cAMP binding was performed as described under "Materials and Methods" on growth stage transformants. PB/AS is the ratio of [^{3}H]cAMP bound in phosphate buffer *versus* that bound in ammonium sulfate (units are $\times 10^3$). Amount of binding is corrected for 8×10^7 cells. AS is the amount of [^{3}H]cAMP bound in ammonium sulfate, and a value of 100 (units, cpm $\times 10^{-3}$) corresponds to 10^5 sites/cell (units, cpm $\times 10^{-3}$). Vector control has AS binding of 31 ± 24. The values show the average ± S.E. of one to five experiments done in triplicates. The *open line* in the chimera diagrams indicates the cAR1 sequence, the *solid line* represents the cAR2 sequence, and the *gray bar* represents the membrane domain. Nomenclature for the chimeras is explained under "Materials and Methods."

Chimeras	PB/AS	AS	Chimeras	PB/AS	AS
cAR1	41 ± 3	332 ± 97	272C	30 ± 3	131 ± 79
cAR2	9 ± 1	399 ± 199	245C	20 ± 10	92 ± 36
N302	63 ± 8	457 ± 313	223C	9	155
N272	21 ± 5	346 ± 124	199C	14 ± 4	195 ± 161
N228	39 ± 1	380 ± 10	177C	ND	ND
N173	52 ± 12	223 ± 114	169C	15	104
N121	5 ± 2	426 ± 70	148C	60 ± 15	202 ± 143
N91	16 ± 6	217 ± 70	139C	123 ± 30	110 ± 10
N82	10 ± 0	359 ± 204	106C	96 ± 2	130 ± 33
N45	20 ± 5	121 ± 14	45C	70 ± 32	260 ± 82

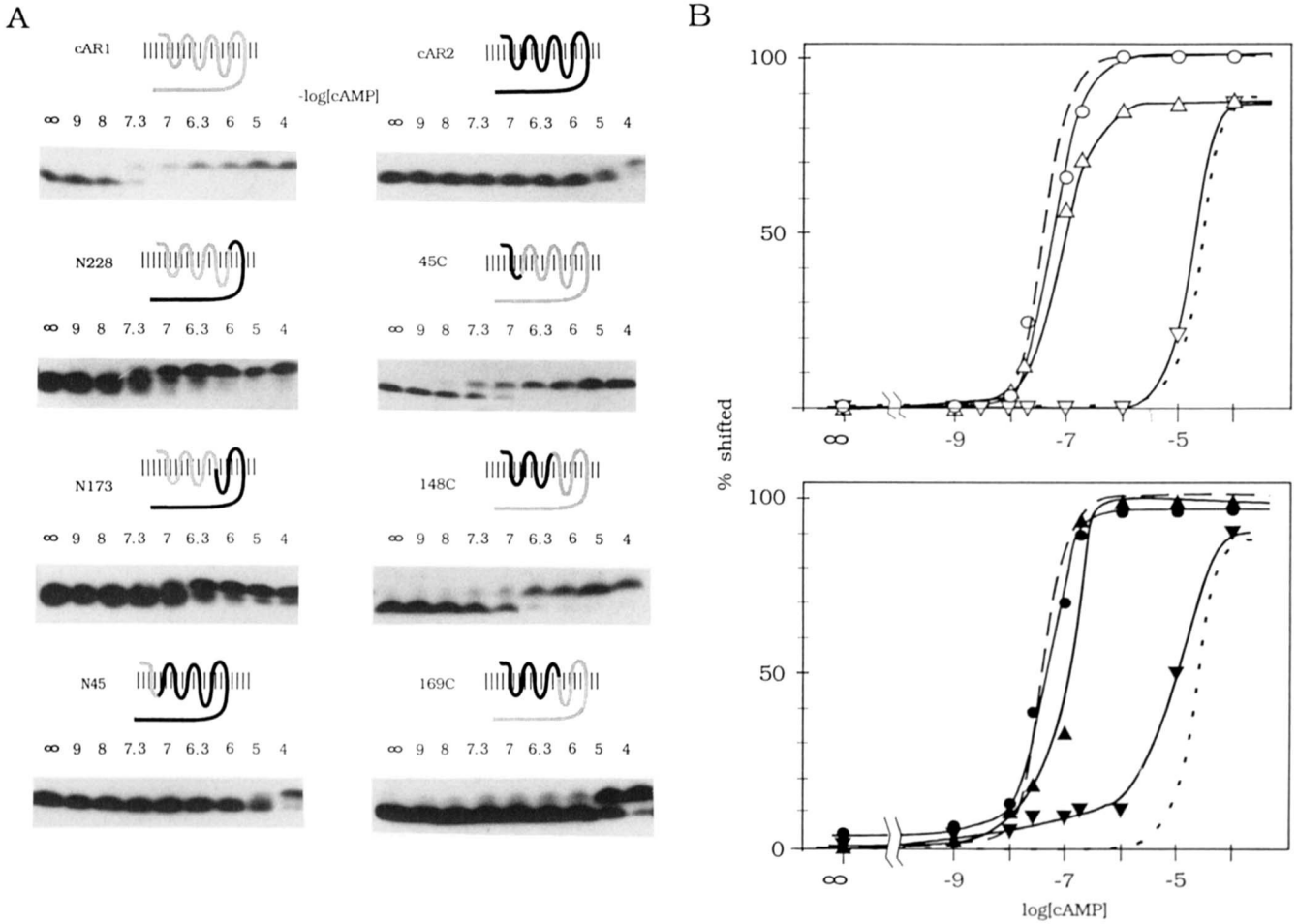

FIG. 2. **Effect of cAMP concentration on electrophoretic mobility shift of chimeras.** The dose dependence of electrophoretic mobility shift assay was performed as described under "Materials and Methods." *A*, whole cell samples treated with indicated dose of cAMP were analyzed on SDS-polyacrylamide gel electrophoresis, immunoblotted with either cAR1- or cAR2-specific rabbit polyclonal antisera, and visualized with chemiluminescence. *B*, graph showing the quantitated results of the dose curve of electrophoretic mobility shift of *A*. *Open* and *filled symbols* represent N and C series, respectively. ○, N228; △, N173; ▽, N45; ●, 45C, ▲, 148C; ▼, 169C. *Dashed lines* indicate the wild-type cAR1 dose curve, and the *dotted line* indicates the curve for wild-type cAR2. Data points are the average value of one to five experiments.

Immunoblotting—Whole cells were solubilized in Laemmli sample buffer (35) and protein samples (10^6 cell equivalent) were analyzed by SDS-polyacrylamide gel electrophoresis using 10% acrylamide and 0.05% bisacrylamide (36). Immunoblots were performed as described previously using either cAR1- or cAR2 COOH terminus-specific rabbit polyclonal antiserum (36). Primary antibodies were detected with either ^{125}I-protein A (DuPont NEN) or alkaline phosphatase-conjugated donkey anti-rabbit-IgG antibodies and chemiluminescence (Amersham Corp.).

cAMP Binding Assays—cAMP binding assays were performed in either PB or in the presence of ammonium sulfate (AS). Cells were resuspended at 10^8/ml in ice-cold PB, and cAMP binding was measured in PB containing 16 nM [^{3}H]cAMP and 10 mM dithiothreitol at 0 °C as described (37). The AS binding assay was performed in 3 M ammonium sulfate with 25 nM [^{3}H]cAMP and 10 mM dithiothreitol as described (37).

Electrophoretic Mobility Shift Assay—The receptor electrophoretic mobility shift assay was performed as described (38). Briefly, cells were resuspended at 3×10^7/ml in ice-cold PB and shaken at 200 rpm with 5 mM caffeine for 20 min at 22 °C to produce the unmodified form of the receptors. Cells were then stimulated with the indicated doses of cAMP with 10 mM dithiothreitol and shaken at 200 rpm for 10 min.

Scatchard Analysis—Vegetative stage cells expressing chimeras were washed and resuspended to 10^8/ml in ice-cold PB. cAMP binding using [^{32}P]cAMP (34) was performed in triplicate in the presence of varying amounts of non-radioactive cAMP as described (37).

RESULTS

Generation of the Random Chimera Libraries—To determine the structural domains that confer high affinity binding of cAMP, we generated libraries of cAR1/cAR2 chimeras as well as cAR2/cAR1 chimeras by random chimeragenesis (Fig. 1). Plasmids containing cAR1 and cAR2 in tandem in the desired order were linearized between the two inserts and transformed into competent JM101 cells. The transformation efficiency was greatly reduced compared with that of the intact plasmid but higher than linear plasmid containing a single insert, about 2000 colonies appeared when 1 μg of DNA were used. Eighteen clones of each directional library were arbitrarily selected and sequenced to locate the position of crossover (see "Materials and Methods"). Most of the chimeras crossed over at some point along the seven transmembrane domains or the intervening loop regions. The homology between the two receptors is greatest here, and only one crossover occurred outside of this region in a homologous part of the cytoplasmic tail.

The process of random chimeragenesis occurs with high fidelity. All of the chimeras were in the correct reading frame and contained no deletions, insertions, or double crossovers; all produced proteins with appropriate carboxyl-terminal tails as assessed by immunoblotting with COOH-terminal specific antisera. Although the mechanism by which random chimeragenesis occurs is not clearly understood, it occurs in a recA$^-$ background and therefore is considered to be independent of recombination.[3] Subsets of the chimeras were selected and transferred to an expression vector. The chimeras were selected

[3] R. Reed, personal communication.

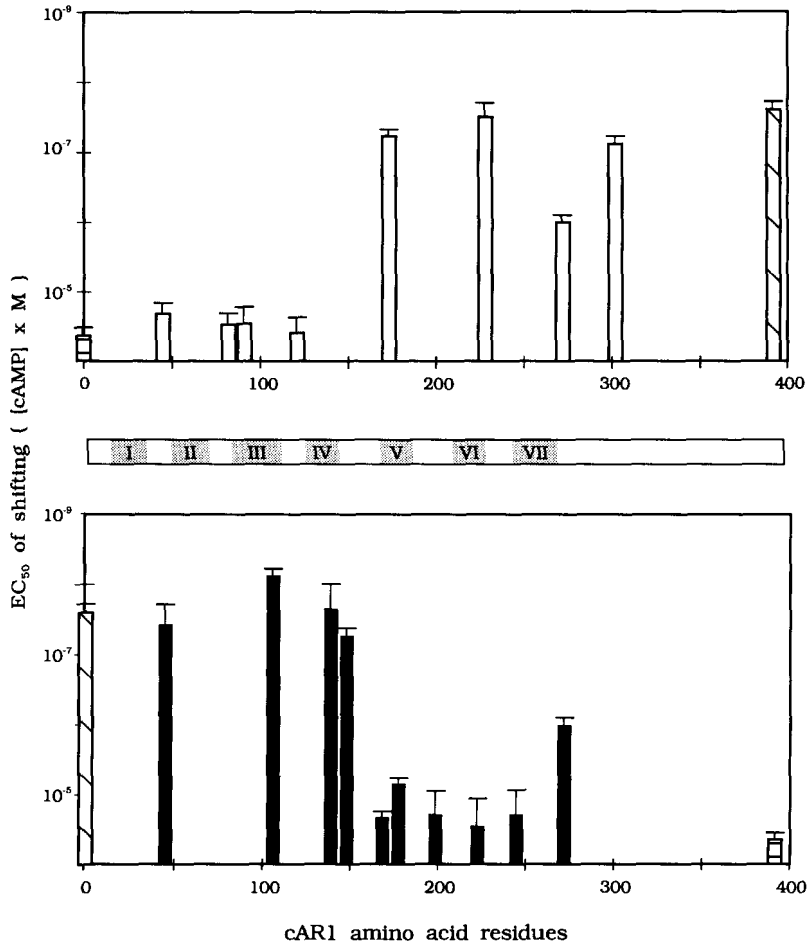

FIG. 3. **EC_{50} of electrophoretic mobility shift of chimeras.** The electrophoretic mobility shift experiments were carried out as described in the legend to Fig. 2. The EC_{50} value of each chimera is plotted on the *y* axis *versus* the point of crossover (in reference to cAR1 amino acid residues). In the *bar model* of cAR1, Roman numerals indicate the seven transmembrane domains. *Open bars* in the histogram indicate chimeras in the N series (1/2 chimeras), and *filled bars* indicate chimeras in the C series (2/1 chimeras). *Bars* with *slanted hatched* marks represent wild-type cAR1, whereas *cross-hatched bars* represent wild-type cAR2. The values obtained are the average ± S.E. of two to six experiments.

so that there would be at least one chimera in each direction that crossed over at each of the seven transmembrane domains, and there would be closely corresponding sets in each direction (Table I).

The Wild-type cAR1 and cAR2 Receptors—Under physiological conditions (10 mM phosphate buffer) a large difference in affinity is observed between cAR1 and cAR2 (Table I). cAR1 displays two classes of affinities, high (25 nM) and low (230 nM), whereas the affinity of cAR2 is too low for binding to be detected within the limits of the assay (>5 μM). The enormous affinity difference of the two receptors is essentially eliminated when the binding is carried out in the presence of 3 M ammonium sulfate. Under these conditions the affinity of cAR1 and cAR2 are 4 and 11 nM, respectively (27).

Fig. 2 illustrates the shift in electrophoretic mobility of cAR1 and cAR2. For cAR1 the electrophoretic mobility shift is due to the phosphorylation of serine residues within a cluster extending from residues 299 to 304 within the cytoplasmic tail (39). Two of these serines are conserved in cAR2 and may cause the mobility shift in cAR2 (25). The EC_{50} values for this response are 30 nM for cAR1 and 50 μM for cAR2 (Fig. 2), which reflects the large affinity differences.

cAMP Binding to the Chimeras—The constitutive expression of the chimeric receptors provided by the actin-15 promotor enabled us to perform the biochemical characterization of the chimeric receptors in growth stage cells in the absence of a significant endogenous wild-type receptor background (33). After stably transformed cell lines were established, the capacity of each chimera to bind at a single concentration of cAMP was tested. By carrying out the binding assay with 25 nM [^{3}H]cAMP (a saturating dose in AS) in the presence of 3 M ammonium sulfate, we assessed the functional integrity of each chimera. By carrying out the assay under physiological conditions in phosphate buffer with a low concentration of [^{3}H]cAMP (16 nM), we detected the high affinity binding sites typical of cAR1 (27).

As shown in Table I, all of the receptors bound a significant amount of [^{3}H]cAMP in the presence of 3 M ammonium sulfate, demonstrating that all were functional and high affinity. Binding in phosphate buffer revealed different classes of chimeric receptors. Many chimeras showed typical "cAR1-like" binding (PB/AS ratio > 35), whereas other chimeras displayed only a low amount of binding or nondetectable cAR2-like binding. The ratio of binding in PB *versus* AS corrected for the amount of the receptor expressed in different cell lines on various days (note the errors in AS binding values).

When we compared these values with the putative topology of the cARs, a clear trend was observed in each series of chimeras. As increasingly more cAR2 sequences comprised the NH_2-terminal portion of a chimeric receptor, the apparent affinity switched abruptly from high to low (C series). The transition occurred within a narrow zone, including the COOH-terminal region of the second extracellular loop connecting TM4 and TM5 and the NH_2-terminal region of TM5 (between 148C and 169C). Similarly, as increasing amounts of cAR1 sequence comprised the NH_2-terminal portion of a chimeric receptor (N series), the apparent affinity changes abruptly from low to high across the same narrow domain (from N121 to N173). These results suggest that the COOH-terminal region of the second extracellular loop of each receptor is necessary to achieve its appropriate affinity of agonist binding under physiological conditions.

EC_{50} of the Electrophoretic Mobility Transition—Although cAR1-like chimeras display cAMP binding under physiological conditions, the cAR2-like chimeras do not. Moreover, the single

concentration assay does not provide the magnitude of the affinity differences compared with either of the wild-type receptors. To distinguish more subtle differences in the chimeric receptors, we assessed the EC_{50} for the agonist-induced electrophoretic mobility transition. For cAR1, under physiological conditions, the EC_{50} value of this response appears to reflect its K_d for cAMP binding (27, 29). Although the K_d value of cAR2-like chimeras cannot be assessed in these conditions, the EC_{50} values of the electrophoretic mobility shift can be readily measured (29).

We first chose representative chimeras that displayed each of the affinity classes in the phosphate buffer cAMP binding assay (Fig. 2). All of the chimeras which displayed typical cAR1-like cAMP binding, such as N228, N173, 45C, and 148C, showed low EC_{50} values as expected (30–80 nM). N228 and 45C exhibited EC_{50} values identical to wild-type cAR1 (30 nM), whereas the EC_{50} values of N173 and 148C were 80 nM, slightly higher than wild-type cAR1. In contrast, N45 and 169C, chimeras that did not bind cAMP in phosphate buffer, displayed cAR2-like EC_{50} values (50 μM).

Fig. 3 provides the EC_{50} values of all of the two-part chimeras that we characterized. For cAR1/cAR2 chimeras, the addition of 121 amino acid residues from cAR1 (N121) did not change the EC_{50} value from that of cAR2 (50 μM). When an additional 52 amino acid residues from cAR1 were included (in N173), the EC_{50} value suddenly decreased to 80 nM. Additional cAR1 sequence decreased the EC_{50} value to 30 nM where it was maintained. For the cAR2/cAR1 chimera series, replacing the NH_2-terminal 148 amino acid residues of cAR1 with those of cAR2 slightly increased the EC_{50} value to 80 nM (Figs. 2 and 3). However, replacing 21 additional amino acids with cAR2 sequence switched the EC_{50} of the subsequent chimeras to that of cAR2. These results further implicate the COOH-terminal portion of the second extracellular loop and the beginning of TM5 as a major determinant of the magnitude of EC_{50} as well as binding affinity.

Scatchard Analysis of Representative Chimeras—The data in Table I and Fig. 3 indicate that the COOH-terminal portion of the second extracellular loop and NH_2-terminal portion of TM5 is crucial in determining the affinity and EC_{50}. In the EC_{50} determinations, two chimeras (N173 and 148C) bordering this region displayed slightly higher EC_{50} values than that of cAR1 (80 nM). We performed Scatchard analysis on the chimeras near the boundaries to more accurately determine the affinity (Fig. 4). In this analysis, wild-type cAR1 displayed two affinity sites, with K_d values of 14 and 390 nM, as described previously (27). Mutant N173 also showed two affinity sites but the K_d values were 19 and 990 nM. The increase in K_d in this chimera closely reflects the increase in EC_{50} value we observed. Mutant 148C had a K_d value only slightly higher than that of cAR1 (19 nM, 625 nM), indicating that the EC_{50} and K_d values are not precisely correlated for this chimera. Nevertheless, these results suggest that there is very close link between the K_d and EC_{50} values.

Three-part Chimeras—To further examine whether the regions mapped by inference from the two series of two part chimeras were sufficient to confer the distinctive properties of cAR1 and cAR2, we generated several three-part chimeras by a second round of random chimeragenesis. When we included 63 residues of cAR1, in the cAR2/cAR1/cAR2 chimera containing residues 110–173 of cAR1, the resulting receptor exhibited a cAR1-like binding profile (K_d ≈ 16 nM, 650 nM; data not shown). Forty-five of the residues in this region are conserved; substitution of only 18 residues decreased the EC_{50} value by 3 orders of magnitude (Fig. 5). In addition, the cAR2/cAR1/cAR2 chimera that contains only residues 148–173 from cAR1 had a

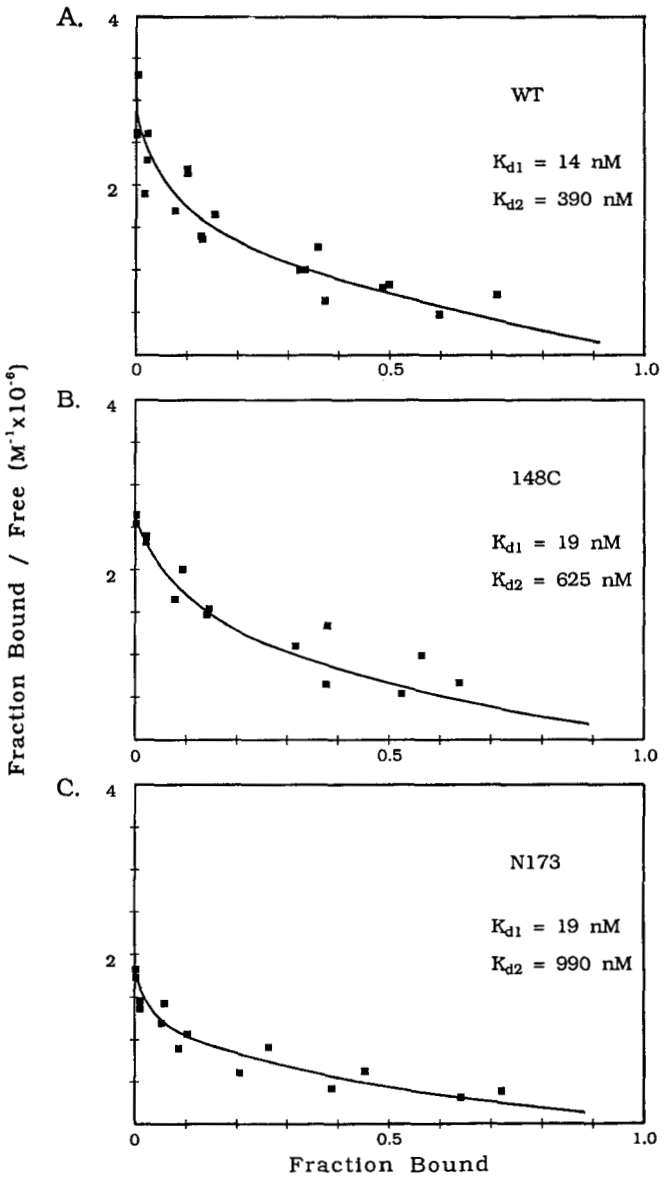

FIG. 4. **Scatchard plots of PB binding of boundary chimeras.** Cells transformed with wild-type cAR1 (*A*), 148C (*B*), and N173 (*C*) were incubated with 1 nM [^{32}P]cAMP and increasing amount of nonradioactive cAMP as described under "Materials and Methods." Means of two to three experiments each in triplicates are shown. The *x* axis was normalized to B_{max} in each case for comparison.

significantly lower K_d and EC_{50} value than cAR2 (Fig. 5). Thus, this region contains the major determinants of affinity. In this region only 7 residues differ between the two receptors. Two are conservative changes in TM5 (L169F and A173G); the rest are in the extracellular loop resulting most notably in the removal of two negative charges (V154D and T157D) that are present in the cAR2 sequence (Fig. 7).

These observations suggest that the additional 11 substitutions present in chimera 110–173 compared with chimera 148–173 are less significant, but allow the receptor to achieve an additional increase in affinity. To confirm this result, we generated two cAR1/cAR2/cAR1 three-part chimeras that replaced either residues 120–149 or residues 120–159 of cAR1 with those of cAR2. As expected, substitution of residues 120–149 only slightly increased the EC_{50} compared with that of wild-type cAR1 to 100 nM (Fig. 6). However, the 120–159 chimera had cAR2-like EC_{50} value, confirming that the residues in the region from 148 to 159 are essential in allowing the formation

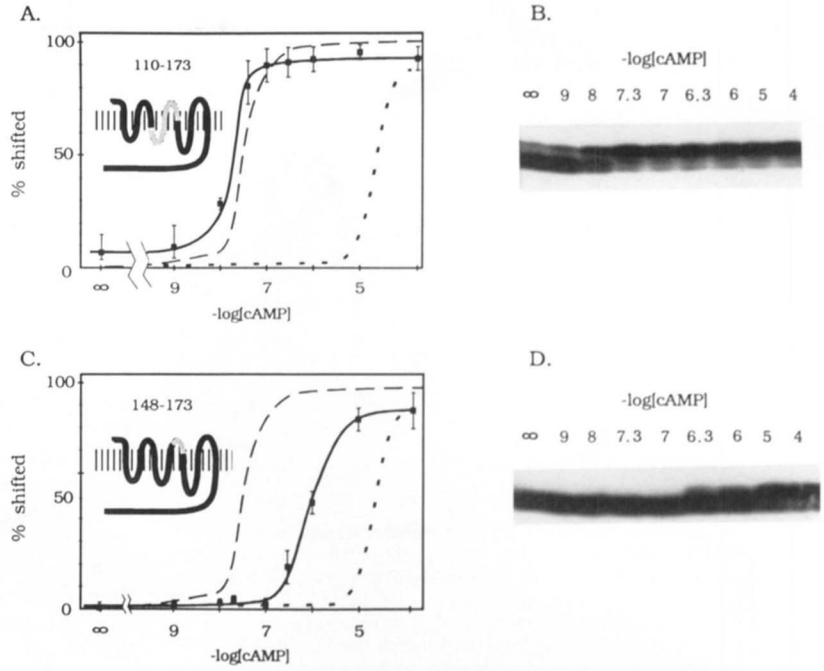

FIG. 5. **cAMP concentration dependence of the electrophoretic mobility shift of cAR2/cAR1/cAR2 chimeras.** Growth stage transformants were treated for electrophoretic mobility shift as described in the legend to Fig. 2. *A*, percent of 2/1/2 chimera, 110–173 (cAR1 with cAR2 sequence from 110 to 173), in higher molecular weight form is shown with a *solid line*; the *dashed line* represents the wild-type cAR1 dose curve and the *dotted line* is that of cAR2. The values are the average ± S.E. of two experiments. *Inset*, putative topology of the 110–173 chimera. The *gray line* indicates the cAR1 sequence, whereas the *black line* represents the cAR2 sequence. *B*, representative immunoblot used to quantitate *A* is shown. The blot was probed with cAR2-specific antisera. *C*, dose curve of electrophoretic mobility of shift in cAR2/cAR1/cAR2 148–173 chimera. The values are the average ± S.E. of two experiments. *D*, corresponding representative autoradiograph of *C*.

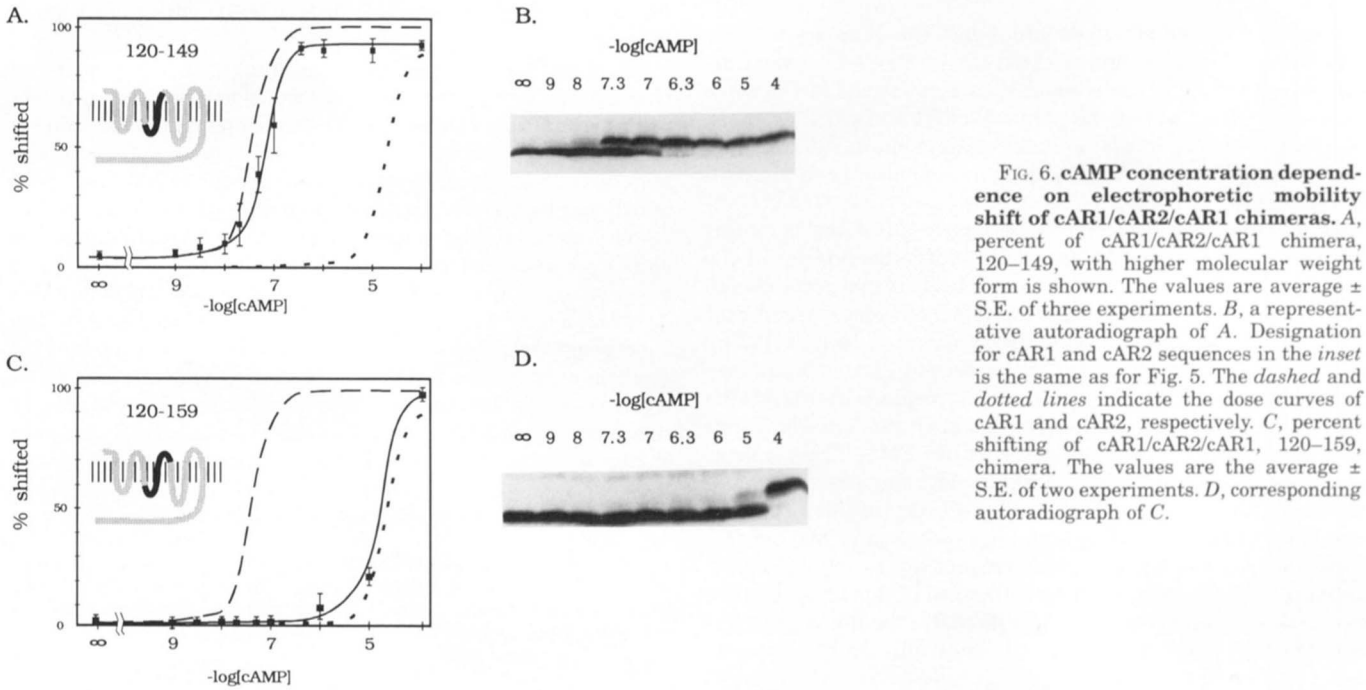

FIG. 6. **cAMP concentration dependence on electrophoretic mobility shift of cAR1/cAR2/cAR1 chimeras.** *A*, percent of cAR1/cAR2/cAR1 chimera, 120–149, with higher molecular weight form is shown. The values are average ± S.E. of three experiments. *B*, a representative autoradiograph of *A*. Designation for cAR1 and cAR2 sequences in the *inset* is the same as for Fig. 5. The *dashed* and *dotted lines* indicate the dose curves of cAR1 and cAR2, respectively. *C*, percent shifting of cAR1/cAR2/cAR1, 120–159, chimera. The values are the average ± S.E. of two experiments. *D*, corresponding autoradiograph of *C*.

of cAR1-like binding characteristics. This latter chimera does not substitute the two conserved residues in TM5, suggesting that these are of little importance in affinity determination.

Two Types of Chimeras That Deviated from the General Trend—There were two types of surprising results revealed in the careful analysis. First, there were two chimeras, 106C and 139C that showed a high level of "constitutive" phosphorylation. Even in the absence of the ligand, a significant amount of these receptors (30–70%) were found in the phosphorylated high molecular weight form (data not shown). The remainder of these receptors underwent the agonist-induced electrophoretic mobility transition with an EC_{50} of 8 nM, a value about 4-fold lower than that of the wild-type cAR1 (Fig. 3). Further characterization of these constitutively phosphorylated chimeras will be presented separately. Second, there were two chimeras (N272 and 272C) that did not follow the trends we have described. The junctions of these chimeras are immediately following TM7 (Table I). These two receptors displayed intermediate affinity in the single concentration phosphate buffer binding assay (Table I) and showed EC_{50} values of 1 μM (Fig. 3). In the case of N272, the EC_{50} value increased from the 30 nM of the surrounding chimeras (N302 and N228), whereas for 272C the EC_{50} value decreased from the 50 μM of the surrounding receptors (cAR2, 245C) to 1 μM (Fig. 3).

DISCUSSION

Random chimeragenesis is a powerful new technique for the functional analysis of homologous proteins. A single transformation with the linearized plasmid containing the two sequences in tandem yielded thousands of independent crossover events. When we screened the libraries for additional chimeras that crossed over within a narrow region, we were able to find

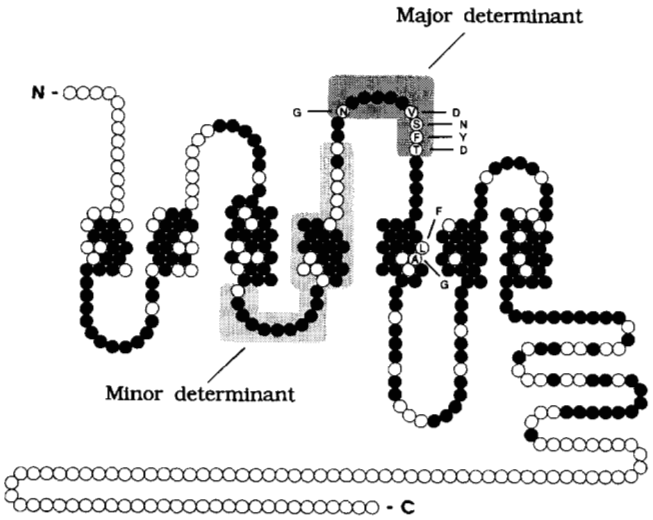

FIG. 7. **Model for the high affinity modulating domains.** The model of cAR1 is shown. *Solid circles* indicate residue identities with cAR2, and *open circles* represent residue differences. Single letter designation of amino acid residues inside of the circle is that of cAR1 sequences and outside of the circle is the corresponding residues in cAR2. The cAR1 residue "*N*" at the 4–5 extracellular loop is residue 148 and "*A*" in TM5 is residue 173.

the desired chimeras, suggesting that the libraries contain nearly every possible chimera that can be formed between the two receptors. All of the chimeras were expressed at the same consistent high level as the parental cAR1 and cAR2 proteins. Most significantly, in the presence of ammonium sulfate, all of the chimeras bound cAMP with a similar affinity of approximately 5 nM.

Under physiological conditions, nearly all of the chimeras behaved as either high or low affinity. The boundaries of the domain that confers high affinity resides between residues 110 and 173. The stretch from 148 to 173, which is most significant for high affinity, consists of 26 amino acids residues, including the COOH-terminal portion of the second extracellular loop and a portion of TM5 (Fig. 7). Nineteen residues in this stretch are identical between the two receptors. Of the 7 residues that differ, two are conserved changes within TM5. These appear insignificant because the cAR1/cAR2/cAR1 chimera, containing residues 120–158 of cAR2, has cAR2-like affinity. Thus a smaller region, from 148 to 159, appears to confer most of this difference. Five of the essential residues are in the 4–5 extracellular loop. The most striking difference in this domain is the presence of two negative charges in cAR2, the low affinity receptor. cAR3, which has an intermediate affinity, has one negative charge in this domain (26). Interestingly, in a random mutagenesis study we have isolated a mutant that converts cAR1 to cAR2-like (*i.e.* low affinity binding under physiological conditions and high affinity binding in ammonium sulfate). This mutant, R160S,H191P, has two point mutations, one of which removes a positive charge from the second extracellular loop.[4]

Chimeras at the boundaries of the high affinity domain, 148C and N173, display an approximately 3-fold increase in EC_{50} values compared with wild-type cAR1 (Figs. 2 and 3). However, not all of this difference is reflected in the dissociation constant. When we performed Scatchard analysis, N173 showed slightly lower than wild-type cAR1 affinities, whereas 148C showed cAR1-like K_d. This discrepancy might indicate that there is small difference between the affinity and EC_{50} determining components; however, they are closely overlapping.

Chimeras 106C and 139C exhibited constitutive phosphorylation and were also hypersensitive. These receptors did not become dephosphorylated even after extensive washing. Even when transformed into *aca*⁻ cell lines that are devoid of endogenous cAMP (40), these receptors still displayed persistent phosphorylation in the absence of exogenous ligand. The persistently phosphorylated state may reflect a constitutively activated conformation which renders them substrates for the receptor kinase.

Curiously, swapping the cytoplasmic tails of the receptors at a point just beyond TM7 results in chimeras that do not bind cAMP characteristically (N272, 272C). These results suggest that the integrity of the transition region between TM7 and the cytoplasmic tail is important in maintaining the proper binding of the agonist. However, at this point the role of this subdomain in determination of affinity of the receptors is not clear.

In order to assess the *in vivo* function of the chimeras, several chimeras were transformed into *car1*⁻ cells, which fail to aggregate upon starvation. The low affinity receptors failed to rescue this phenotype, whereas each of the chimeras that define the boundaries of the high affinity domain (148C and N173) did (data not shown). This result suggests that the intracellular loops and the cytoplasmic tail of cAR2 are sufficient for rescue provided that the receptor binds with high enough affinity.

All of our observations are consistent with the hypothesis that interactions within the 4–5 loop can weaken an intrinsically high affinity interaction. The phenomena of high affinity binding of the cAMP receptors in 3 M ammonium sulfate are not very well understood; however, since all of the receptors bind cAMP and they share extensive homology in the domains that is involved in binding, it is possible that by adding ammonium sulfate we are measuring the maximum "intrinsic affinity" of a given receptor. Each receptor may have similar intrinsic affinity provided by the residues in the plane of membrane. The short segment in 4–5 extracellular loop that we mapped in this study may be involved in the modulation of this intrinsic affinity. We suggest that here we have found a new mode of affinity regulation in which very highly conserved family of receptors change a few amino acid residues to either facilitate or hinder the access of ligand to binding site and achieve a three-magnitude modulation in their affinities for the same ligand.

Acknowledgments—We thank Dr. Charles L. Saxe III for cAR2 genomic DNA and oligonucleotide primers used in this study. We also thank Michael Caterina, Mei-Yu Chen, and Dale Hereld for helpful discussions and Pamela Lilly for critical reading of the manuscript.

REFERENCES

1. Dohlman, H. G., Thorner, J., Caron, M. G., and Lefkowitz, R. J. (1991) *Annu. Rev. Biochem.* **60,** 653–688
2. Gilman, A. G. (1987) *Annu. Rev. Biochem.* **56,** 615–649
3. Birnbaumer, L. (1992) *Cell* **71,** 1069–1072
4. Logothetis, D. E., Kurachi, Y., Galper, J., Neer, E. J., and Clapham, D. E. (1987) *Nature* **325,** 321–326
5. Tang, W. J., and Gilman, A. G. (1991) *Science* **254,** 1500–1503
6. Savarese, T., and Fraser, C. (1992) *Biochem. J.* **283,** 1–19
7. Devreotes, P. N. (1989) *Science* **245,** 1054–1058
8. Devreotes, P. N. (1994) *Neuron* **12,** 1–20
9. Schaap, P., Konijin, T. M., and Van Haastert, P. J. M. (1984) *Proc. Natl. Acad. Sci. U. S. A.* **81,** 2122–2126
10. Williams, J. G., Jermyn, K. A., and Duffy, K. T. (1989) *Development* **107,** (suppl.) 91–97
11. Wang, J. K., McDowell, J. H., and Hargrave, P. A. (1980) *Biochemistry* **19,** 5111–5117
12. Fidlay, J. B. C., Brett, M., and Pappin, D. J. C. (1981) *Nature* **293,** 314–317
13. Kobilka, B. K., Matsui, H., Kobilka, T. S., Yang-Feng, T. L., Francke, U., Caron. M. G., Lefkowitz, R. J., and Regan, J. W. (1988) *Science* **238,** 650–656
14. Strader, C. D., Sigal, I. S., Candelore, M. R., Rands, E., Hill, W. S., and Dixon, R. A. F. (1988) *J. Biol. Chem.* **263,** 10267–19271
15. Wang, C. D., Buck, M. A., and Fraser, C. M. (1991) *Mol. Pharmacol.* **40,** 168–179

[4] J.-Y. Kim, M. C. Caterina, K. C. Lin, and P. N. Devreotes, manuscript in preparation.

16. Khorana, H. G. (1992) *J. Biol. Chem.* **267,** 1–4
17. Tsai-Morris, C. H., Buczko, E., Wang, W., and Dufau, M. L. (1990) *J. Biol. Chem.* **265,** 19385–19388
18. Xie, Y.-B., Wang, H., and Segaloff, D. L. (1990) *J. Biol. Chem.* **265,** 21411–21414
19. Nagayama, Y., Russo, D., Wadsworth, H. L., Chazenbalk, G. D., and Rapoport, B. (1991) *J. Biol. Chem.* **266,** 14926–14930
20. Nagayama, Y., and Rapoport, B. (1992) *Endocrinology* **131,** 548–552
21. Quehenberger, O., Prossnitz, E. R., Cavanagh, S. L., Cochrane, C. G., and Ye, R. D. (1993) *J. Biol. Chem.* **268,** 18167–18175
22. Gao, J. L., and Murphy, P. M. (1993) *J. Biol. Chem.* **268,** 25395–25401
23. Yokota, Y., Akazawa, C., Ohkubo, H., and Nakanishi, S. (1992) *EMBO J.* **11,** 3585–3591
24. Perez, H. D., Holmes, R., Vilander, L. R., Adams, R. R., Manzana, W., Jolley, D., and Andrews, W. (1993) *J. Biol. Chem.* **268,** 2292–2295
25. Saxe, C. L., III, Ginsberg, G. T., Louis, J. M., Johnson, R., Devreotes, P. N., and Kimmel, A. R. (1993) *Genes & Dev.* **7,** 262–272
26. Johnson, R., Saxe, C. L., III, Gollop, Kimmel, A. R., and Devreotes, P. N. (1993) *Genes & Dev.* **7,** 273–282
27. Johnson, R. L., Van Haastert, P. J. M., Kimmel, A. R., Saxe, C. L. III, Jastorff, B., and Devreotes, P. N. (1992) *J. Biol. Chem.* **267,** 4600–4607
28. Milne, J., and Devreotes, P. N. (1993) *Mol. Biol. Cell* **4,** 283–292
29. Johnson, R. L., Gundersen, R., Hereld, D., Pitt, G. S., Tugendreich, S., Saxe, C. L., Kimmel, A. R., and Devreotes, P. N. (1992) *Cold Spring Harbor Symp. Quant. Biol.* **57,** 169–176
30. Klein, P., Sun, T. J., Saxe, C. L., Kimmel, A. R., Johnson, R. L., and Devreotes, P. N. (1988) *Science* **241,** 1467–1472
31. Chen, M.-Y., Devreotes, P. N., and Gundersen, R. E. (1994) *J. Biol. Chem.* **269,** 20925–20930
32. Pitt, G. S., Milona, N., Borleis, J., Lin, K. C., Reed, R. R., and Devreotes, P. N. (1992) *Cell* **69,** 305–315
33. Johnson, R. L., Vaughan, R. A., Caterina, M. J., Van Haastert, P. J. M., and Devreotes, P. N. (1991) *Biochemistry* **30,** 6982–6986
34. Caterina, M. J., Milne, J. L. S., and Devreotes, P. N. (1994) *J. Biol. Chem.* **269,** 1523–1532
35. Laemmli, U. K. (1970) *Nature* **227,** 680–685
36. Klein, P., Vaughan, R., Borleis, J., and Devreotes, P. (1987) *J. Biol. Chem.* **262,** 358–364
37. Van Haastert, P. J. M. (1985) *Biochim. Biophys. Acta* **845,** 254–260
38. Vaughan, R. A., and Devreotes, P. N. (1988) *J. Biol. Chem.* **263,** 14538–14543
39. Hereld, D., Vaughan, R., Kim, J.-Y., Borleis, J., and Devreotes, P. (1994) *J. Biol. Chem.* **269,** 7036–7044
40. Pitt, G. S., Brandt, R., Lin, K. C., Devreotes, P. N., and Schaap, P. (1993) *Genes & Dev.*. **7,** 2172–2180